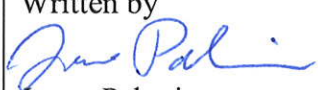
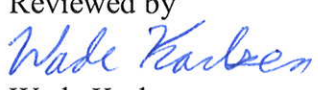
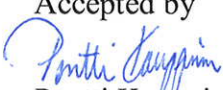




(S)TEM analysis of OFP copper CT-tested in S containing groundwater

Authors: Janne Pakarinen

Confidentiality: Public

Report's title (S)TEM analysis of OFP copper CT-tested in S containing groundwater	
Customer, contact person, address KYT2014 Research Programme and SSM	Order reference
Project name CuHa	Project number/Short name 73775 /CUHA2011
Author(s) Janne Pakarinen	Pages 17/
Keywords Copper, sulphur, transmission electron microscopy	Report identification code VTT-R-04957-11
<p>Summary</p> <p>OFP CT-sample tested in sulphur containing (200 mg /l) groundwater was examined by using (S)TEM-EDS. The specimens were fabricated from the close proximity of the fracture surface, which previously has been shown by SEM-EDS to contain up to 20 at% of S. STEM-EDS maps and TEM-EDS point analyses showed that the Cu matrix contained a varying amount of sulphur rich particles and traces of phosphorus segregation on the grain boundaries. It was assumed that the majority of the S-rich particles had fallen out during electrolytic sample preparation, leaving behind matrix with a varying density of holes. One open grain boundary was found to contain corrosion product with Cl and other elements relevant to the groundwater environment. Reference samples which had not been in contact with groundwater nor strained also showed P segregation at the grain boundaries and S rich particles.</p> <p>Most notably, particle density seemed to vary by location in the CT-tested samples. While some grains were nearly particle free, some had significant amount of particles. It was suggested that the amount of precipitates was related to the stress state of each grain during the CT-test. According to theoretical calculations in the literature, S forms stable and mobile defect complexes with vacancies. In the selective dissolution, vacancy creep model, vacancies on the other hand are believed to be injected in to the material during corrosion and annihilate during deformation. High stress in grains, which are in preferential orientation to straining axis would then, hypothetical, lead to larger injection of vacancies and diffusion of S via mobile S-vacancy defects. Further research by using novel methods, such as atom probe tomography, is proposed to tackle that problem.</p>	
Confidentiality	Public
Espoo 1.7.2011 Written by  Janne Pakarinen Research Scientist	
Reviewed by  Wade Karlsen Senior Scientist	
Accepted by  Pentti Kauppinen Technology Manager	
VTT's contact address Kemistintie 3, Espoo; P.O. Box 1000, FI-02044 VTT, Finland	
Distribution (customer and VTT)	
<i>The use of the name of the VTT Technical Research Centre of Finland (VTT) in advertising or publication in part of this report is only permissible with written authorisation from the VTT Technical Research Centre of Finland.</i>	

Preface

This report summarizes the transmission electron microscopy work done in the KYT2014 research project “CuHa”.

Espoo 1.7.2011

Authors

Contents

Preface	2
1 Introduction.....	4
2 Description.....	4
3 Methods.....	5
4 Results	6
4.1 Reference samples	6
4.2 CuHa1 and CuHa5.....	11
5 Discussion and Conclusions.....	16
6 Summary	16
7 Bibliography.....	17

1 Introduction

In Scandinavia, copper has been proposed to be the material from which the outer layer of cast iron canisters for the final repository of nuclear waste are to be made (Posiva, SKB). The canisters will be buried deep into the bedrock and embedded in bentonite clay. The choice of copper for the barrier material is natural in the sense that the properties of copper have been known since the Iron Age. The canisters are expected to sustain a predefined lifetime of (at least) 100,000 years. During the 100,000 years, the copper canisters will be exposed to decay heat of the spent fuel and groundwater environment. To sustain the integrity of the capsule, the corrosion rate of the copper must be well known. Another important aspect is related to the mechanical properties, most notably the susceptibility of copper to stress corrosion cracking (SCC) in groundwater.

Grain boundaries play a key role in intergranular cracking of copper. Basically, substitute atoms weaken the cohesion of the boundary and increase the possibility of cracking upon applied stress. There are findings in the literature that segregation of certain elements on copper grain boundaries may enhance intergranular fracture. T. Nieh and W. Nix found that oxygen enhances intergranular (IG) fracture (1), while G. Ducher et al. found that bismuth segregation at the grain boundaries also leads to increased embrittlement (2).

The role of sulphur in the SCC of copper is still a subject of debate, even though it has been shown to increase SCC susceptibility in some cases(3). In the case of copper canisters, the exposure to S is possible via bacterial activity or/and transport via ground water (4). Furthermore, there are several post-fracture investigations clearly showing that the IG fracture surface is covered with sulphur (5)(6). Theoretical investigations have shown that the solubility of S in Cu is very limited due to formation of the stable Cu_2S phase (7). Theoretically the S should form highly stable and mobile S-vacancy and S-S defect complexes that favour the precipitation of Cu_2S to lattice defects (dislocations, grain boundaries, open surfaces, etc).

Despite being experimentally assumed and theoretically predicted, no atomic-scale experimental results on S segregation on the copper grain boundaries have been reported to date. The main goal of this research was to examine the role of S on SCC of copper.

2 Description

The examined specimens were extracted from a Compact Tension (CT) –test piece, which was tested in saline ground water containing $[\text{S}^{2-}] = 200 \text{ mg/l}$. The test details and optical/SEM investigations on the fracture surface can be found from (8). Macro images from the examined regions are shown in Fig. 1 (a) and (c). There are black spots at the fractured surface, as shown in Fig. 1 (a), which according to SEM-EDS analyses were composed mainly of S. TEM specimens (CuHa1 and CuHa5) were punched from the locations shown in Fig. 1 (b) and (d). As a reference, TEM samples were also fabricated from material, which had not been in contact with the ground water environment. Altogether seven reference

samples were fabricated during optimization of the electrolytic polishing process and three of those (Ref3, Ref4, and Ref7) were examined by TEM.

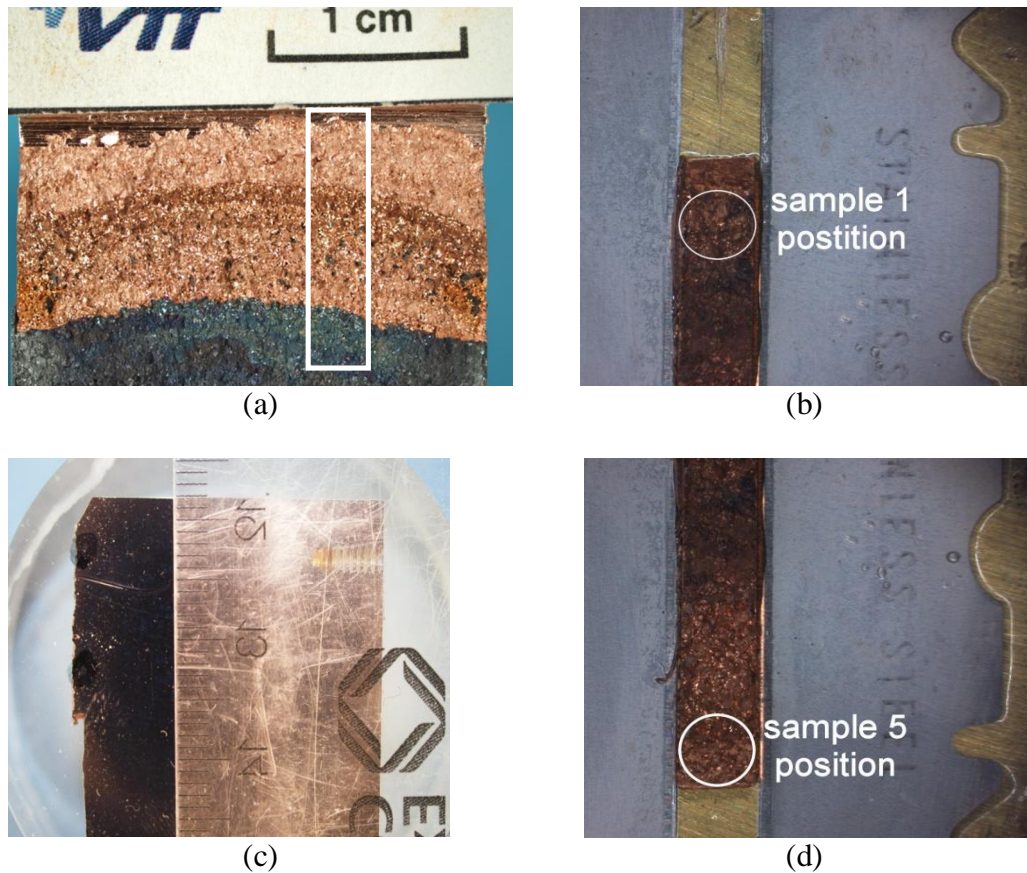


Fig. 1. Macro images of the examined sample. The fracture surface and side view of the C- sample are shown in (a) and (c), while the positions of TEM specimens CuHa1 and CuHa5 are shown in (b) and (d). The white box in (a) shows the approximate position of which samples were punched. The white circles in (b) and (d) are 3 mm in diameter.

3 Methods

The blanks for the specimens were first cut by a diamond blade saw and then manually ground to a thickness of 300 μm . TEM specimens were then punched from the ground blanks [according to Fig. 1 (b) and (d)] and further grinded to a thickness below 100 μm . The specimens were then electrolytically polished to electron transparency by using automatic Tenupol polishing unit and phosphorus-acid based Struers D2 electrolyte (6 V, about 50 mA). A Philips CM200 FEG Scanning transmission electron microscope (STEM) was used to explore the chemistry of particles and grain boundaries in close proximity to the cracked surface (~ 0.3 mm below) of the CT-sample. The spot size used for EDS analysis was $\sim 1\text{nm}$.

4 Results

4.1 Reference samples

The general appearance of the examined samples Ref3 and Ref4 is shown in Fig. 2. Most distinctly, all the examined samples showed a large amount of holes that were most likely a consequence of particles dropping out during the electrolytic polishing procedure. There was no evidence that the amount of holes would have been larger at the grain boundaries as compared to the matrix.

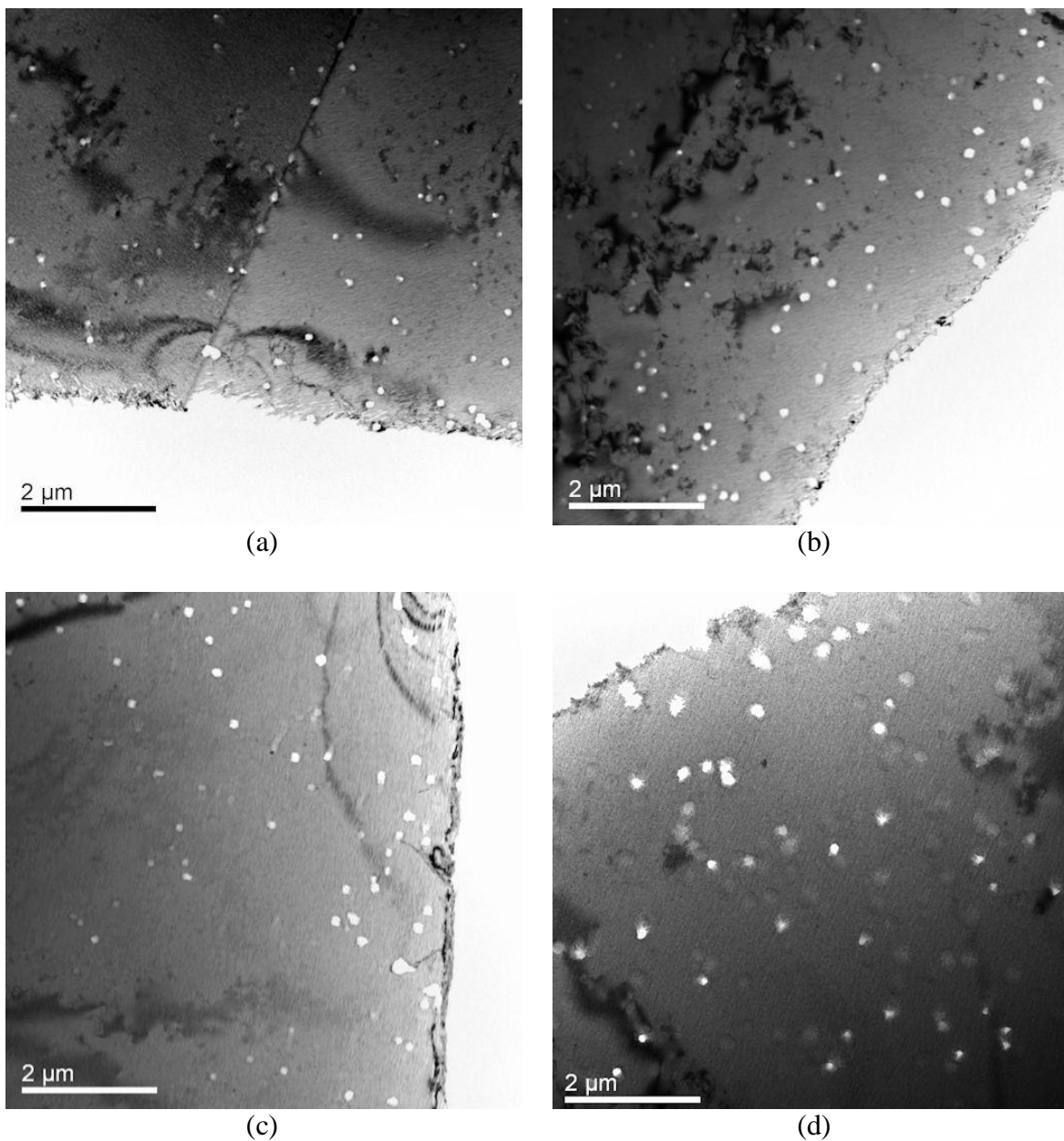


Fig. 2. General appearance of Ref 3 [(a) and (b)] and Ref 4 [(c) and (d)]. The matrix showed a varying distribution of apparent inclusions that were fallen off during electrolytic

polishing of specimens.

To verify that the holes did not contain any impurities, STEM-EDS maps from the location of fallen particles was done. As shown in Fig. 3 indeed, there were no impurities at the fall out locations. Notice that the reverse contrast between Figs. 2 and 3 is due to STEM images taken in high-angle annular dark field (HAADF) mode. HAADF contrast is especially sensitive to changes in elemental composition. The linear vertical feature in Fig. 3 is a grain boundary, and the contrast variation between the two grains is due to different lattice orientations. The size of the particles was a couple of hundred nanometers.

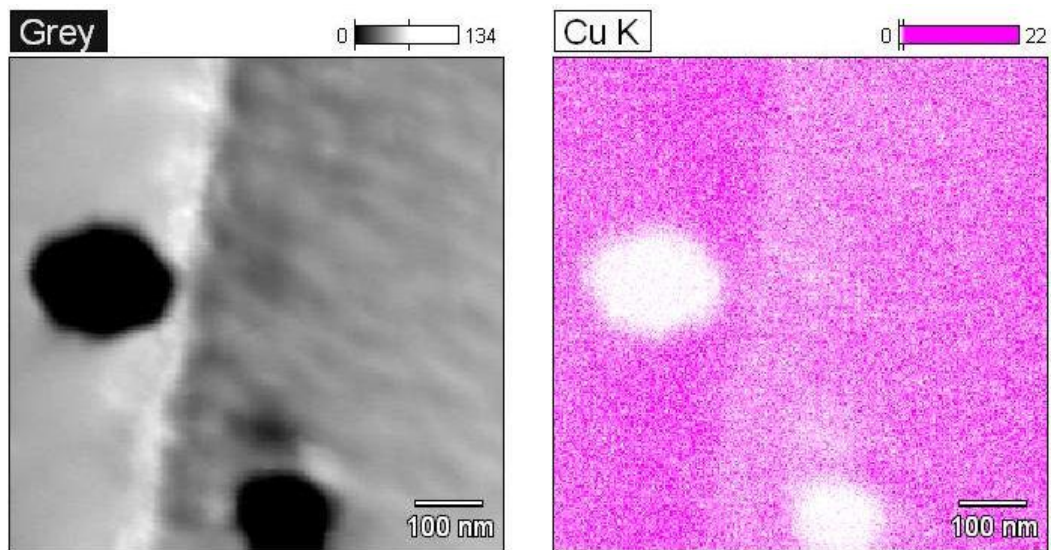


Fig. 3. STEM-EDS map of a region in Ref3 where couple of inclusions have fallen off from the matrix.

As is also noticed from Fig. 3, the grain boundary did not show any significant signs of segregated elements, although according the experience it would be difficult to see low concentration in a STEM-EDS map. Further examination on grain boundaries were made by using spot analyses.

In some locations, precipitates were found and analyzed by using spot analyses and STEM-EDS. Figs. 3 and 4 show STEM-EDS maps of some of the particles. In general, these particles were found in random locations. Most commonly they were sitting on the edge of a hole left by a particle that had fallen out, as shown in Fig. 5. According to the STEM maps, the particles clearly contained copper, sulphur and phosphorus. To get a more precise compositional analysis of the particles, point analyses were taken from a variety of precipitates. Results from the analyses are collected to Table 1.

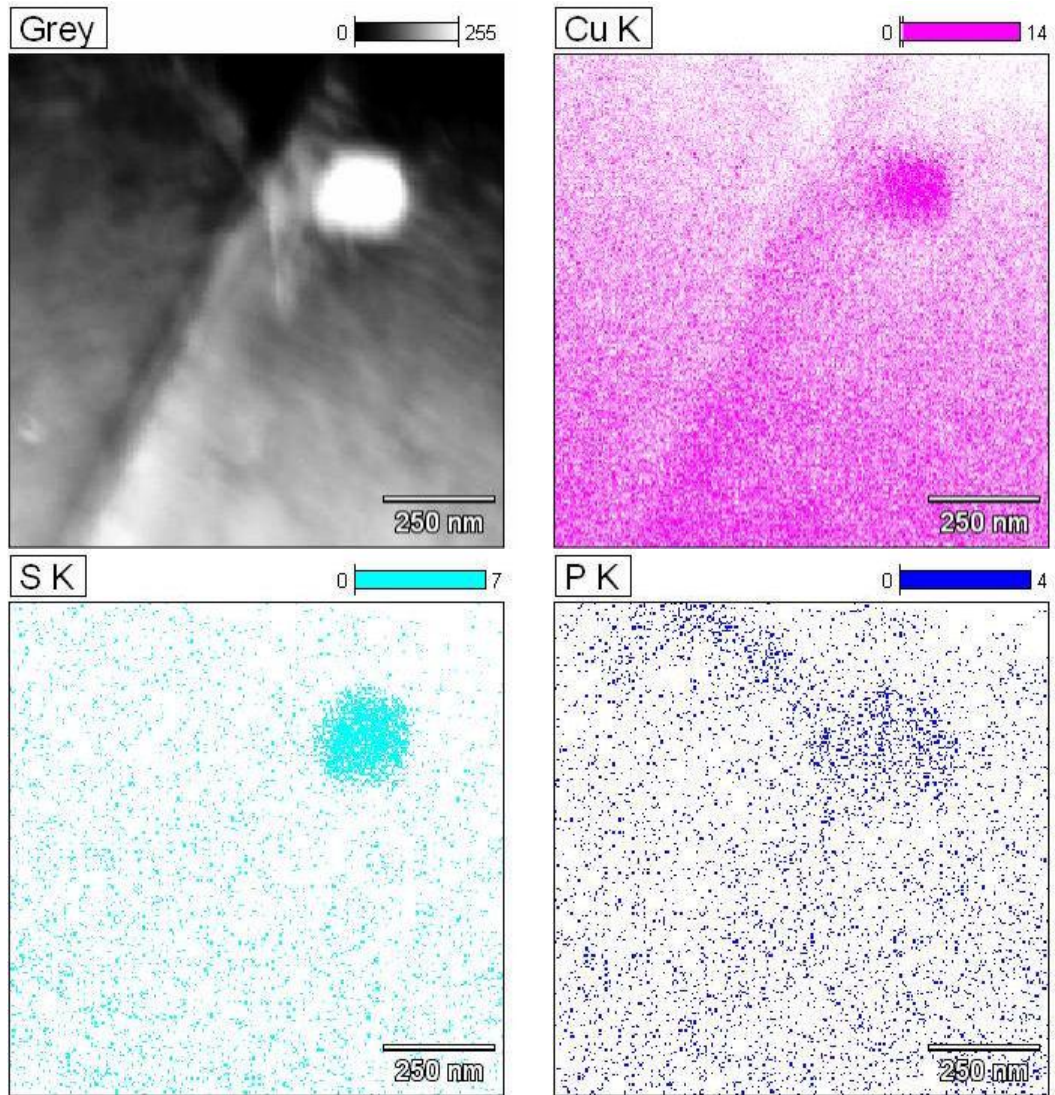


Fig. 4. Particle in Ref 3 foil edge. Clear signs of Cu, S and P detected by STEM-EDS.

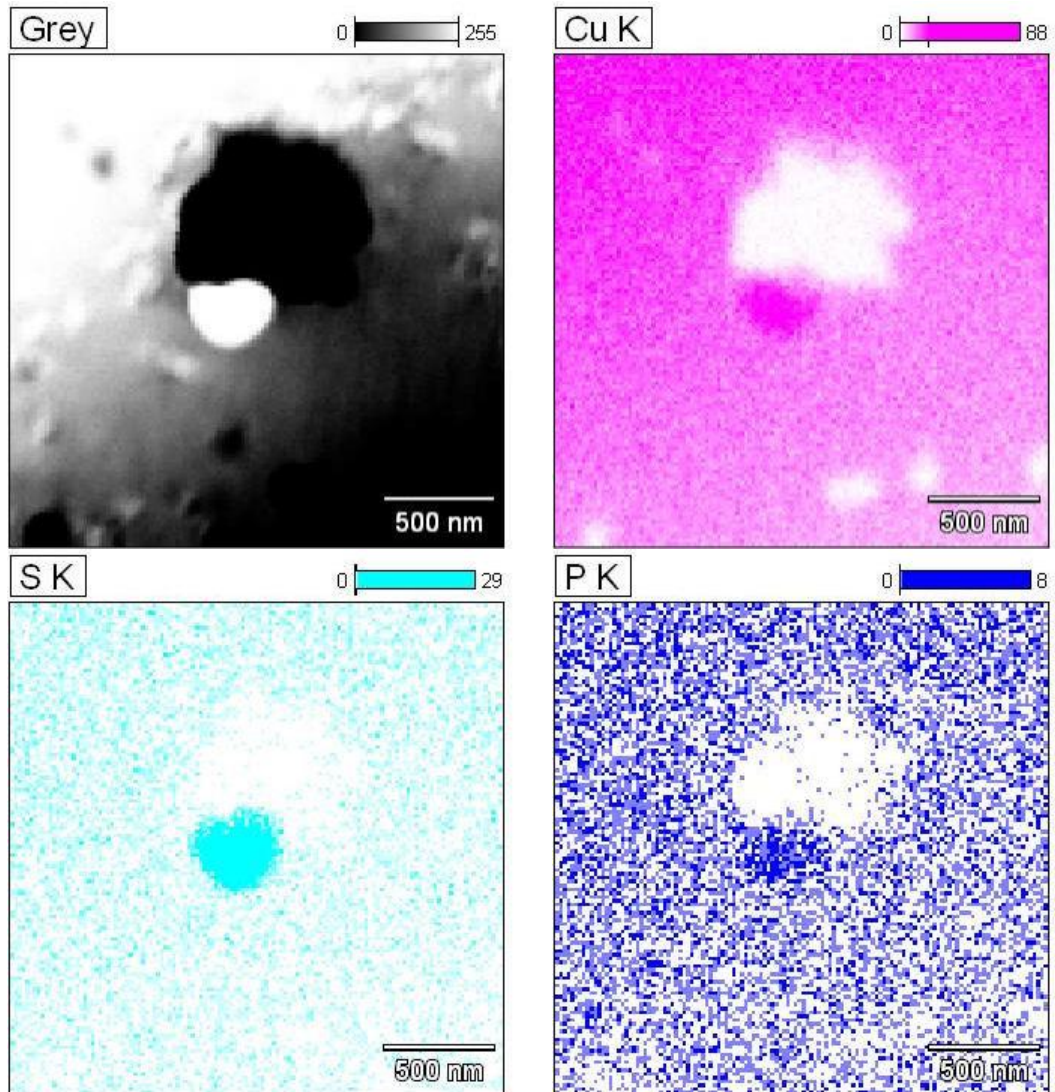


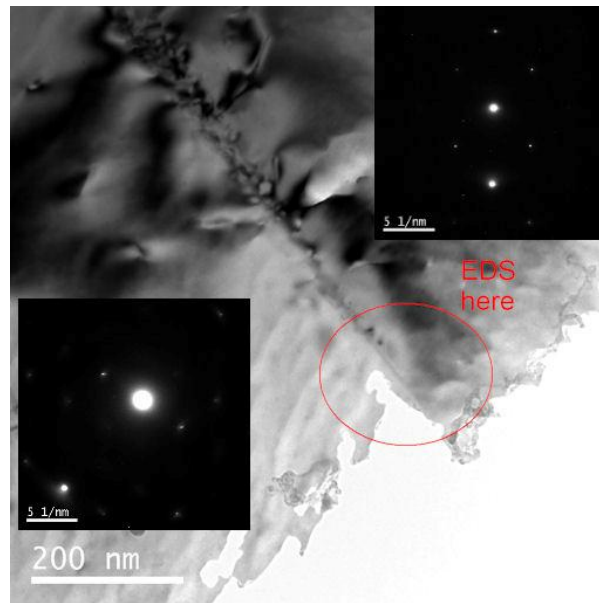
Fig. 5. Particle sitting at the edge of the hole in Ref 4. The particle clearly contains S and some P.

Table 1. Weight percentages of the examined precipitates of Ref3, Ref4, and Ref7.

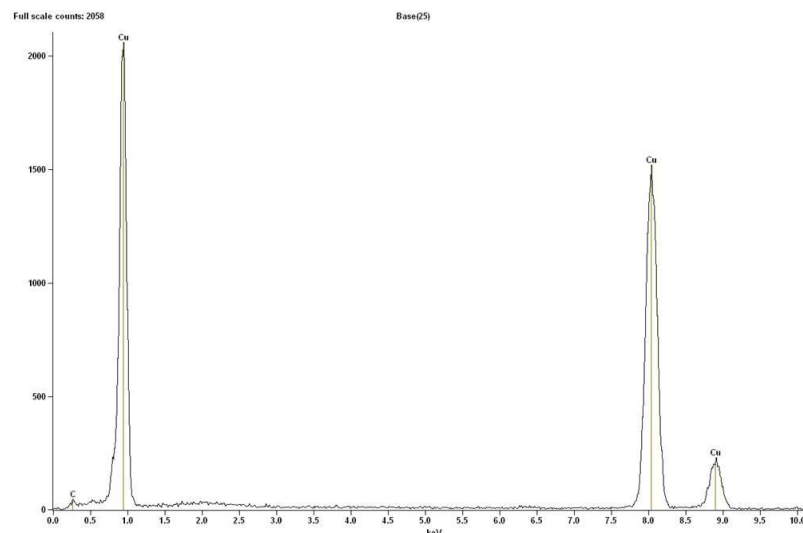
#	Cu wt%	S wt%	P wt%	Si wt%	Cl wt%
EDS3_11	balance	21.1	0.6	-	-
EDS4_1	balance	23.5	-	-	-
EDS4_4	balance	-	0.8	-	-
EDS4_5	balance	-	2.3	-	-
EDS4_6	balance	21.7	0.1	-	-
EDS4_8*	balance	-	0.3	43.6	0.2
EDS4_10*	balance	-	-	46.9	-
EDS4_11	balance	0.3	0.6	-	-
EDS7_51	balance	22.4	0.1	-	-
EDS7_52	balance	14.1	0.9	-	-
EDS7_53	Balance	18.9	0.6	-	-

*) One individual particle containing high Si was found from one examined foils.

Several grain boundaries of the reference samples were examined by using spot analyzes. Fig. 6 shows one of the analysed GBs. Selected area diffraction (SAD) patterns from the neighbouring grains show that there's a difference in crystal orientation, as expected. EDS spot analyses from the region shown inside the red circle in Fig. 6 did not show any impurities at the GB. A representative EDS spectrum shown in Fig. 6 (b) contains only a weak peak from C contamination and clear emissions related to Cu.



(a)

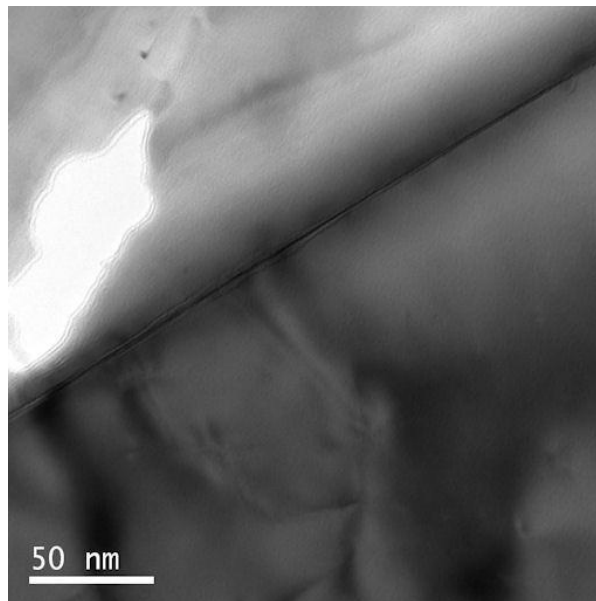


(b)

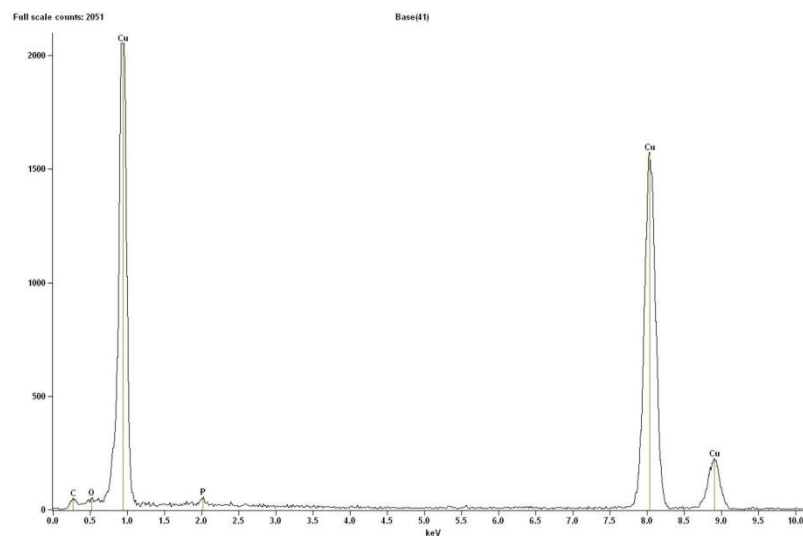
Fig. 6. Grain boundary analyzed by using a small probe and EDS. (a) shows the examined region, while (b) shows a representative EDS spectrum (nothing but Cu and C contamination present) from the GB.

Another grain boundary of Ref7 showed a weak but observable signal of phosphorus on the grain boundary. The amount of phosphorus ranged from 0.5 to

1 % wt. The examined region as well as one of the obtained EDS spectra is shown in Fig. 7.



(a)



(b)

Fig. 7. Another grain boundary analyzed by using a small probe and EDS. (a) shows the examined region, while (b) shows a representative EDS spectrum.

4.2 CuHa1 and CuHa5

Specimens for CuHa1 and CuHa5 were fabricated from the proximity of the fracture surface of the CT-sample, as described earlier in Section 2. Specimen CuHa1 was from the first fractured region, while CuHa5 was from the last fractured region. The general appearance of the microstructures in CuHa1 and CuHa5 closely resembled that observed in the reference samples. A large amount of holes was found as a consequence of apparent falling out of particles from the matrix.

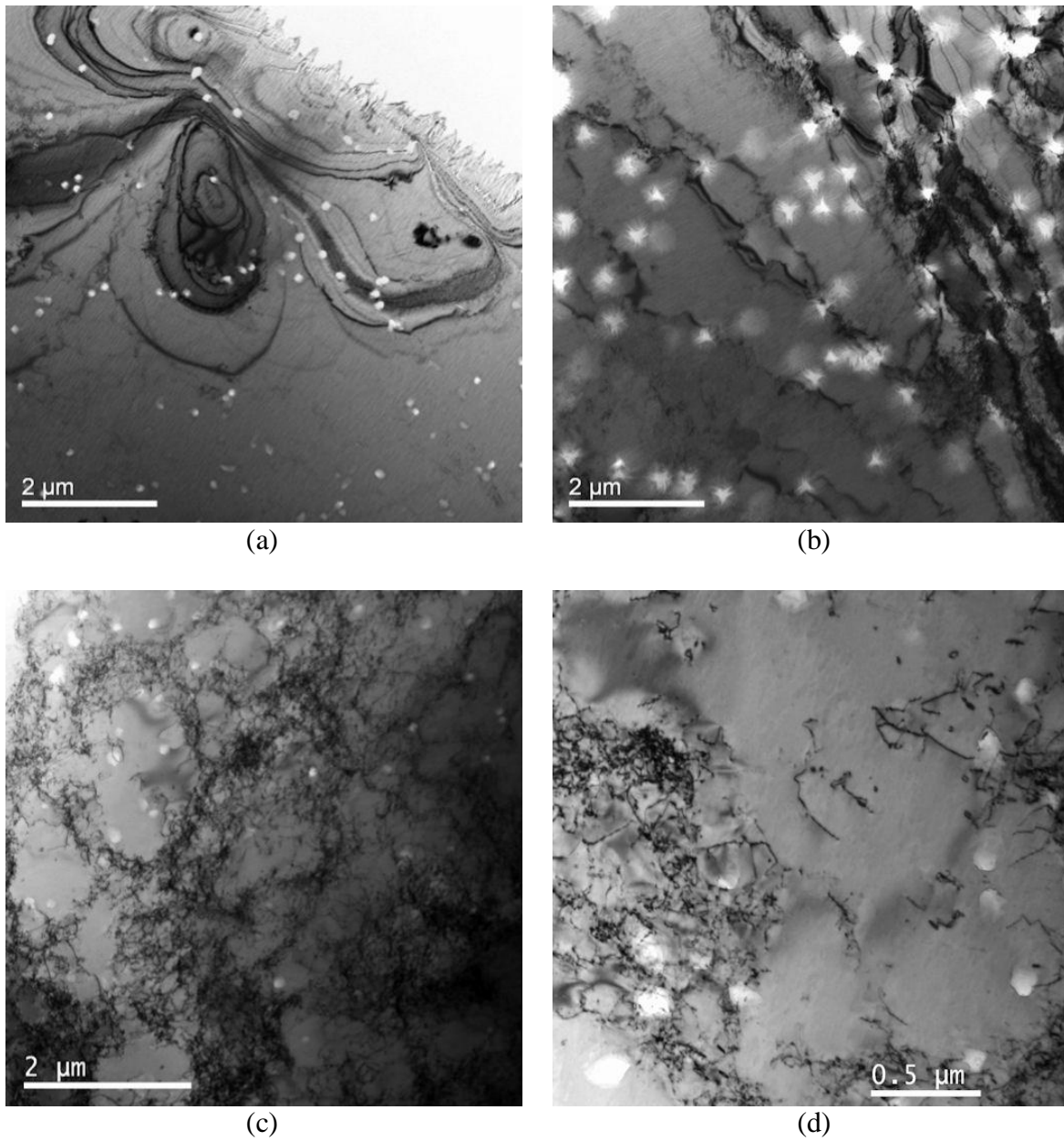


Fig. 8. General appearance of the matrix showed a varying distribution of apparent particles that fell out during electrolytic polishing of the specimens.

As compared to the reference samples, the general impression was that locally some of grains were filled with a larger number of holes/particles, while other grains showed lower density. A comparison between two separate regions from CuHa1 is shown in Fig. 9.

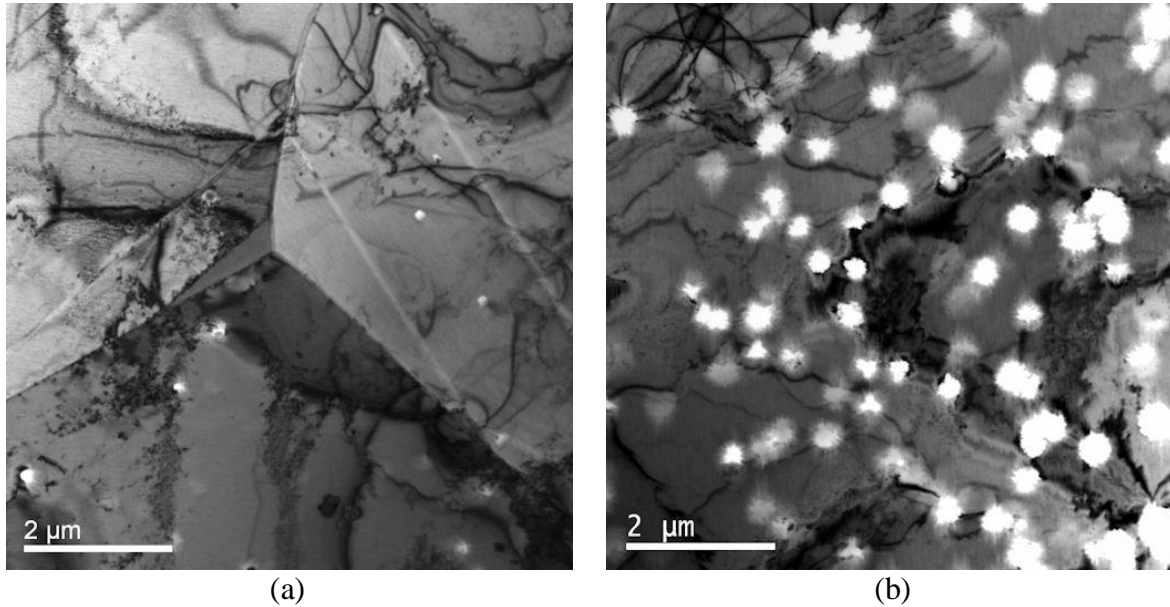
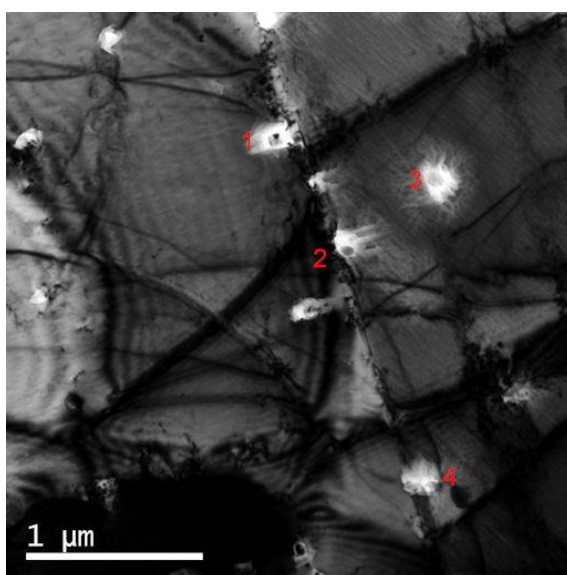


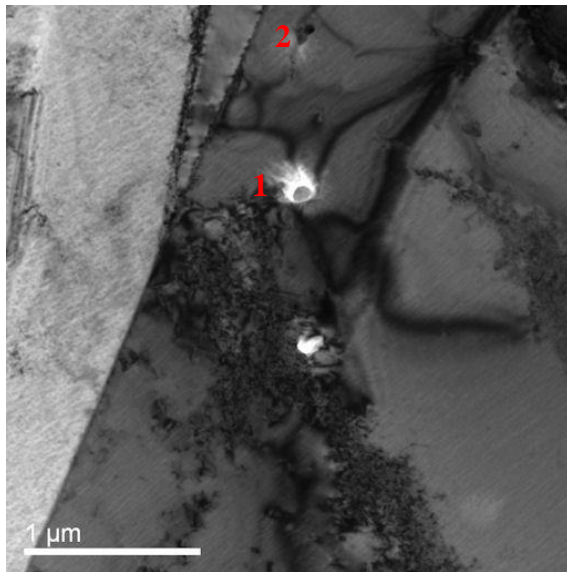
Fig. 9. The amount of holes/particles showed large variation between different regions of CuHa1.

Again, some residual particles were found in the CuHa1 and CuHa5 samples from the edges of the holes left from larger particles falling out. Point analyses from CuHa1 in Fig. 10 show that the particles are composed of high amount of S, but at these points P was not detected. Some of the precipitates are on the grain boundary, but there's no clear trend in that behavior. In addition to S containing precipitates, some triangular features containing Cl were found from CuHa1. The EDS location and the triangular appearance of the Cl containing feature are shown in Fig. 11. Similar S rich particles were found from CuHa5 sample, but Cl containing features were not found.



#	Cu wt%	S wt %	P wt %
1	balance	23.3	-
2	balance	7.3	-
3	balance	3.8	-
4	balance	5.4	-

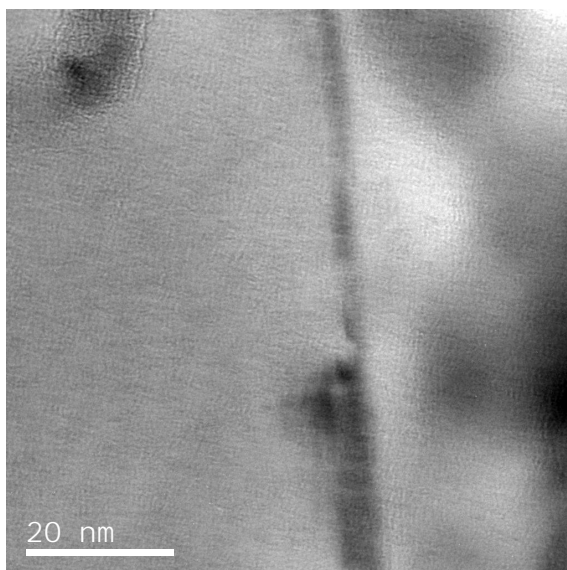
Fig. 10. EDS point analyses and results from CuHa1. The precipitates clearly contain S. No traces of P were found.



#	Cu wt%	S wt %	Cl wt %
1	balance	17.1	-
2	balance	-	3.6 - 6.7

Fig. 11. EDS point analyses and results from CuHa1. The lower precipitate clearly contains S, while Cl was found from the upper feature. No traces of P were found.

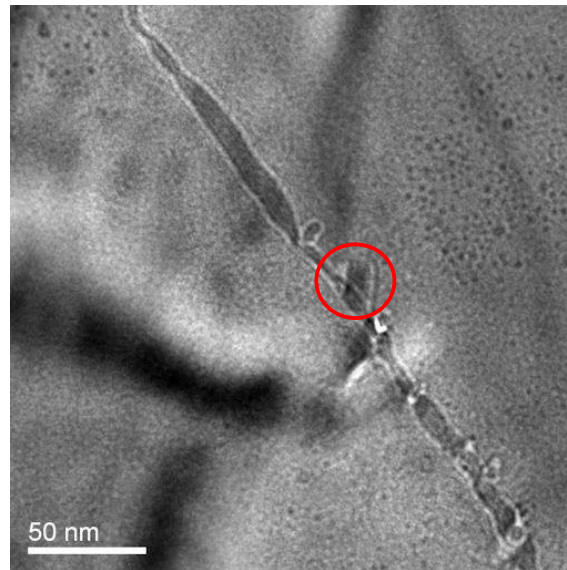
Several grain boundaries of CuHa1 and CuHa5 were examined by using EDS spot analyses. The analysis revealed that the grain boundaries contained small amounts of P but no S, as was also noticed in the reference samples. As an example, one GB of CuHa5 is shown in Fig. 12 with EDS results.



#	Cu wt%	P wt %
1	balance	0.8
2	balance	0.8
3	balance	0.6
4	balance	0.4
5	balance	0.1
6	balance	1.6
7	balance	0.6
8	balance	0.6
9	balance	1.2
10	balance	0.5
11	balance	0.8
12	balance	0.3
13	balance	0.5
14	balance	-
15	balance	0.2

Fig. 12. EDS point analyses and results from CuHa5 grain boundary.

Although most of the boundaries did not show any unfamiliar features, one grain boundary of CuHa1 was clearly filled with some corrosion product, as shown in Fig. 13 with EDS results.



#	Cu wt%	S wt%	Cl wt%	P wt%	K wt%	Cr
1	balance	6.1	1.1	0.5	0.3	3.3
2	balance	2.7	0.9	0.5	0.3	1.6
3	balance	6.2	0.9	0.4	0.2	3.4
4	balance	7.0	0.4	0.3	0.1	3.5
5	balance	0.1	0.3	0.2	0.1	-
6	balance	0.1	0.9	0.3	0.3	-
7	balance	-	1.8	1.6	0.4	-
8	balance	0.2	0.8	0.3	0.2	-
9	balance	0.1	0.7	0.4	0.1	-
10	balance	-	0.8	0.3	0.2	-
11	balance	0.1	0.7	0.3	0.3	-
12	balance	0.1	0.6	0.5	0.3	-
13	balance	-	0.5	0.2	0.2	-
14	balance	-	0.7	0.1	0.2	-
15	balance	0.1	0.8	0.3	0.2	-
16	balance	-	1.1	0.3	0.2	-

Fig. 13. EDS point analyses and results from CuHa1 grain boundary, which clearly was filled with some corrosion product. Locations 1 – 4 are from the circled particle. All the other particles are from the grain boundary. Most notably, there is a S rich particle on the boundary (# 1 -4) and Cl is found everywhere.

5 Discussion and Conclusions

A clear sign of small particles was found from all the examined samples. Due to electrolytic sample preparation, the majority of these precipitates had fallen out in the electron transparent region of the foil and leaving a copper matrix filled with holes. The particles were usually a few hundred nanometers and contained most notably S and some amount of P. While the particle density was rather even in the examined reference samples, the CT-tested samples tend to have large variation in precipitation concentrations.

Grain boundaries have been proposed to be the major diffusion path of S to the copper matrix under applied stress in S containing environment. In the present study, one grain boundary clearly contained corrosion product with Cl and other elements possibly originating from the groundwater.

To explain the SEM and Auger observations of the literature (6)(8), there must be a mechanism for S to diffuse into the fracture surface of the cracked samples. On the other hand, there's a large difference in the resolution of previously mentioned methods as compared to TEM, and thus the smallest precipitates seen by TEM (few nanometres) are far below the detection limit of SEM-EDS. The limit of detection is not, however, able to explain the concentration of S being affected by the strain (8). Likewise, TEM may not be the best method for examining the mechanisms of S diffusion in the Cu lattice at an atomic scale, due to the image always being a projection of a ~100nm thick foil. During the last couple of years the strengths of atom probe tomography (APT) have been indisputably shown to tackle elemental problems in nanometres scale in 3D (9) and the technique would definitely give more insight into this problem as well.

Vacancies are easy to invoke because they are extremely difficult to detect and naturally involved in crack formation and propagation. In the selective dissolution, vacancy creep model it is postulated that corrosion processes at the materials surface can result in an increase in the vacancy flux from surface oxide to metal. In the theoretical examination of P. Korzhavyi,(7) the found possibility of mobile and stable S-vacancy pair in copper, indeed, sounds fascinating possibility to explain the increased amount of sulphur on the fracture surfaces. The fact that different grain had different amount of precipitates could then be related to different strain levels due to different grain orientations. The grains with higher stress would then accompany more S-vacancy pairs, which would then favour the Cu_2S precipitation in these grains.

6 Summary

Copper CT-specimens tested in S containing groundwater were analysed by using (S)TEM. It was found that all the examined samples contained small S rich precipitates. A small amount of P was found from the grain boundaries of both, mechanically tested and reference samples. The mechanism for S diffusion in the Cu lattice was discussed shortly based on experimental findings and literature.

7 Bibliography

1. *Embrittlement of Copper Due to Segregation of Oxygen to Grain Boundaries.* **T.G. Nieh, W.D. Nix.** 1981, Metallurgical Transactions A, pp. 893-901.
2. *Bismuth-Induced Embrittlement of Copper Grain Boundaries.* **G. Dusher, M.F. Chisholm, U. Alber, M. Ruhle.** 2004, Nature Materials, pp. 621-626.
3. *Influence of Sulfide Concentration on the Corrosion Behavior of Pure Copper in Synthetic Seawater.* **N. Taniguchi, M. Kawasaki.** 2008, Journal of Nuclear Materials, pp. 154-161.
4. *Analysis of Copper Corrosion in Compacted Bentonite Clay as a Function of Clay Density and Growth Conditions for Sulfate-Reducing Bacteria.* **Pedersen, K.** 2010, Journal of Applied Microbiology, pp. 1094-1104.
5. *Sulphide Induced Stress Corrosion Cracking of Copper - Final Report.* **E. Arilahti, L. Carpén, T. Lehtikuusi, M. Olin, T. Saario, P. Varis.** 2011, VTT Research Report, pp. VTT-R-00467-11.
6. *Low Temperature Creep of Copper Intended for nuclear Waste Containers.* **P. Henderson, J.-O. Österberg, B. Ivarsson.** 1992, SKB Technical Report, pp. TR 92-04.
7. *Theoretical Investigation of Sulfur Solubility in Pure Copper and Dilute Copper-Based Alloys.* **P. Korzhavyi, I. Abrikosov, B. Johansson.** 1999, Acta Materials, pp. 1471-1424.
8. *Sulphide Induced Stress Corrosion Cracking of Copper - Intermediate Report 3.* **E. Arilahti, T. Lehtikuusi, T. Saario, P. Varis.** 2010, VTT Research Report, pp. VTT-R-10541-10.
9. *Novel Features of Radiation-Induced Segregation and Radiation-Induced Precipitation in Austenitic Stainless Steels.* **Z. Jiao, G.S. Was.** 2011, Acta Materialia, pp. 1220-1238.